Review Article

Challenges in imaging assessment following liver stereotactic body radiotherapy: pitfalls to avoid in clinical practice

Connie Yip[1], Gary J. R. Cook[2,3], Kasia Owczarczyk[2], Vicky Goh[2,4]

[1]Department of Radiation Oncology, National Cancer Centre Singapore, Singapore 169610, Singapore; [2]Division of Imaging Sciences & Biomedical Engineering, Department of Cancer Imaging, King's College London, St Thomas' Hospital, London, UK; [3]Clinical PET Imaging Centre, [4]Department of Radiology, Guy's and St Thomas' NHS Foundation Trust, St Thomas' Hospital, London, UK

Contributions: (I) Conception and design: C Yip; (II) Administrative support: None; (III) Provision of study materials or patients: C Yip; (IV) Collection and assembly of data: C Yip; (V) Data analysis and interpretation: C Yip; (VI) Manuscript writing: All authors; (VII) Final approval of manuscript: All authors.

Correspondence to: Dr. Connie Yip. Department of Radiation Oncology, National Cancer Centre Singapore, 11 Hospital Drive 169610, Singapore. Email: connie.yip.s.p@singhealth.com.sg.

Abstract: Stereotactic body radiotherapy (SBRT) is increasingly used in the management of unresectable liver metastases and hepatocellular carcinoma (HCC) as it allows delivery of high-dose conformal radiotherapy with limited toxicities. However, it may be difficult to differentiate viable tumour from radiotherapy-related changes after SBRT. The imaging changes observed after SBRT may also differ from those observed following conventionally fractionated radiotherapy. Hence, we aim to review the imaging changes that occur within the tumour and adjacent normal liver after SBRT which may help to identify local relapse in clinical practice.

Keywords: Liver; stereotactic body radiotherapy (SBRT); CT; magnetic resonance imaging (MRI)

Submitted Apr 26, 2017. Accepted for publication May 15, 2017.
doi: 10.21037/cco.2017.06.06
View this article at: http://dx.doi.org/10.21037/cco.2017.06.06

Introduction

The introduction of stereotactic body radiotherapy (SBRT) has shifted the paradigm in the management of solid malignancies by enabling the delivery of highly conformal and targeted high-dose hypofractionated radiotherapy with excellent local control rates and minimal toxicities in the appropriately selected patient population (1). Although this technique has been used for intracranial irradiation ("radiosurgery") for many years, its use in extracranial sites was initially limited by the lack of good quality image guided tumour localization/delivery and the ability to deliver highly conformal radiotherapy without damaging normal tissues. This changed with the advent of intensity-modulated radiotherapy (IMRT), the use of CT/MRI for radiotherapy planning and treatment verification, as well as motion management.

SBRT is increasingly used in the management of unresectable liver metastases and hepatocellular carcinoma (HCC) (2-5) as it allows the delivery of ablative radiation doses with limited toxicities. Typically, a total of 30–60 Gy is delivered over 3–6 fractions using highly conformal non-coplanar beams or arc therapy. The prescribed radiation dose is dependent on a multitude of patient and tumour factors (e.g., liver function, number of lesions) as well as risk of normal tissue toxicities. Tumour and liver appearances after SBRT may differ from conventionally fractionated radiotherapy due to the potentially different radiobiological effects on the tumour and normal tissues (6). Most of these radiobiological changes were also evaluated in preclinical models and uncertainty exists regarding the extrapolation of the preclinical dose fractionations used to the clinical setting due to the different doses used, and the biology of murine and human models. Hence, we will review the histopathological and imaging changes that occur following liver SBRT, which may be informative in improving our

post-treatment image surveillance programme and our ability to distinguish normal tumour response from disease progression.

Histopathological changes

Understanding the underlying biological and histological changes is important to allow interpretation of the changes seen on various imaging methods. Most of the evidence for the underlying histopathological radiation-induced changes has been derived from conventionally fractionated radiotherapy in non-cirrhotic liver. These features include hyperaemia, central vascular congestion with fibrin deposition and subsequent collagen formation as well as hepatic cell loss, known as veno-occlusive disease (VOD) (7-9). These changes tend to spare the larger veins and are typically observed between 1–4 months after radiation (7). In most cases, liver hyperaemia and hepatic cell atrophy tend to resolve after 4 months with some residual architectural lobular distortion (7,9).

Olsen *et al.* evaluated the histological changes in two patients who underwent surgical metastasectomy at 2 and 8 months after liver SBRT (10). Both patients received 60 Gy in 3 fractions. Despite the 6 months interval between the two specimens, three distinct zones of radiation induced changes were identified on both specimens. The central zone (zone I) contained central necrosis with fibrosis and scattered macrophages. Zone II was the capillary-rich repopulation zone with areas of fibrosis and granulation tissue, surrounded by regenerating hepatocytes. The outer zone III showed characteristics of VOD with central vein occlusion and marked sinusoidal congestion. There was a clear demarcation between irradiated and non-irradiated liver. Bile ducts were spared in all three zones. At 8 months, there was complete central vein obliteration by collagen fibers in zone III with less congestion and atrophy of the liver cell plates compared to that observed at 2 months.

Focal liver reaction (FLR)

Several imaging studies have reported the morphological and physiological changes observed in the immediate surrounding liver parenchyma receiving non-ablative radiation dose, known as FLR. Overall, normal liver volume decreased following liver SBRT (10). A median normal liver volume reduction of 18% (13–33%) was found at 2–6 months after SBRT in 15 patients with liver metastases (10). In a separate study using [^{18}F]Fluorodeoxyglucose positron emission tomography (FDG PET/CT), there was an average 20% reduction of liver volume at 3–6 months after SBRT for liver metastases. Although regeneration occurred after 12 months, the liver volume remained 10% less than baseline (11).

In addition, a difference in the irradiated and non-irradiated liver density has been observed after SBRT. Generally, a decrease in computed tomography (CT) density of 7–10 Hounsfield units (HU) between irradiated and non-irradiated liver is considered significant (12-14). The SBRT dose associated with a significant reduction in CT density was estimated to be between 30 to 35 Gy in 3–5 fractions (13,15,16) although a lower threshold dose had also been suggested (median calculated threshold dose 13.7 Gy in a single fraction; range, 8.9–19.2) (12). There is also a suggestion that an inverse relationship between SBRT dose and post-treatment normal liver CT density exists (13). However, there is no conclusive evidence that FLR observed after SBRT is related to the development of radiation-induced liver disease (RILD).

Yamasaki *et al.* first reported CT changes in 31 patients with HCCs, cholangiocarcinomas and liver metastases treated with high-dose fractionated conformal radiotherapy (48–73 Gy in 1.50–1.65 Gy twice daily fractions) (17). They found that the treated volumes adjacent to the tumours became hypodense on contrast-enhanced CT in 74% of the patients at 1–4 months post-treatment. In contrast, in the two patients with fatty infiltration, the treated volume showed increased density compared to the untreated liver. These changes did not correlate with the development of radiation hepatitis. Subsequent liver atrophy was observed in four patients, hypertrophy of uninvolved liver in another four patients and both effects were found in eight patients.

Herfarth *et al.* described three types of FLR in 36 patients (1 HCC, 3 cholangiocarcinomas, 32 metastases) who were treated with single fraction SBRT (median dose 22 Gy; range, 16–24) (12). Median follow-up for this cohort was 8.3 months (range, 1.3–17.9 months) after SBRT. Hypodense liver reaction was found in 58% of follow-up unenhanced CT scans compared to non-irradiated liver with a median density difference of –15 HU (range, –10 to –30 HU). However, a third of scans showed no density difference between irradiated and non-irradiated liver. The authors classified the FLR changes into three types based on the density observed in the portal-venous and delayed phase scans: hypodense/isodense (Type 1), hypodense/hyperdense (Type 2) and isodense or hyperdense/hyperdense (Type 3). The median time to development of FLR was 1.8 months

(range, 1.2–4.6) and more than half (64%) of the patients developed type 1 reactions at the first occurrence. However, there was a shift to type 2 and 3 reactions at subsequent follow-up. The volume of FLR decreased at 2–4 months compared to the initial reaction volume (median 40%; range, 17–94%). In the previous study by Olsen *et al.*, a comparison was made between the radiological Herfarth Type 1 and 2 reactions, and the corresponding pathological findings (10). They showed that the hypodensity in the portal-venous phase observed in Type 1 reaction was associated with tissue congestion and occlusion of small veins resulting in decreased perfusion, hence contrast inflow. In contrast, the hyperdensity observed in Type 2 reaction was hypothesised to be secondary to progressive fibrin deposition and occlusion of the central veins causing stasis and pooling with reduced contrast clearance.

In a separate study by Sanuki-Fujimoto *et al.*, three classifications of FLR following SBRT (30–40 Gy in 5 fractions) for HCC in a background of cirrhosis were described (18). In this study, transarterial chemoembolization (TACE) was performed prior to SBRT. Most of the patients had Child-Pugh A cirrhosis. The group identified three FLR density patterns based on the pre-contrast, arterial and portal-venous phase scans: isodense/isodense/isodense (Type A), hypodense/isodense/isodense (Type B) and hypodense/isodense or hyperdense/hyperdense (Type C). These changes occurred at a median of 3 months (range, 1–6 months) after SBRT. When Type A and B reactions were grouped as "unenhanced" as opposed to the "enhanced" Type C reaction, the authors found that livers with preserved function tend to be well enhanced in the delayed phase.

These observations were supported by another study by Kimura *et al.* which evaluated the changes in dynamic CT after SBRT (48 Gy in 4 fractions) for HCC in patients with Child-Pugh A and B liver cirrhosis (19). The majority of patients also underwent TACE prior to SBRT. Dynamic CT was performed in non-contrast, arterial, portal and venous phases. The CT density changes were classified into three types: Type 1—hyperdensity in all enhanced phases, Type 2—hypodensity in arterial and portal phases and Type 3—isodensity in all enhanced phases. This study found that half of Type 2 and 3 reactions changed to Type 1, particularly in Child-Pugh A patients. In contrast, Type 2 and 3 reactions remained unchanged in Child-Pugh B patients.

A further study also evaluated the contrast-enhancement changes in the adjacent irradiated normal liver after SBRT for HCC (14). Most patients (69%) were treated with SBRT alone whereas the remaining patients were treated with SBRT and TACE. Pre-contrast, arterial, portal and delayed CT phase images were acquired before, at one, three and six months post-treatment. The irradiated liver showed hypoattenuation compared to non-irradiated liver on non-contrast images in 26% of patients at one month which increased to 79% at 6 months. In contrast, hypervascularity on the arterial phase was seen in 12% of patients at one month which increased to 54% at 6 months. There was little contrast washout on the delayed phase: 2% at 1 month and 0% at 6 months. These contrast enhancement changes were similar between those treated with SBRT alone, and combination of SBRT and TACE.

It is difficult to directly compare these studies due to several key differences such as the different types of liver tumours, treatment received, timing of assessment, CT imaging phases evaluated and contrast administration. Nonetheless, these studies showed that there was a significant change in the irradiated normal liver density compared to non-irradiated liver which tend to resolve over time (*Figures 1*,*2*). Overall, Herfarth Type 1 and 2, Sanuki-Fujimoto Type A and B and Kimura Type 2 and 3 appearances were of the "unenhanced" pattern which was more prevalent in those with impaired liver function (Child-Pugh B). Both studies by Sanuki-Fujimoto *et al.* and Kimura *et al.* showed that Child-Pugh score was a significant factor associated with the types of imaging changes observed (18,19). However, only Kimura *et al.* showed that non-type 3 changes were associated with higher risk of adverse events (P=0.003) on univariate analysis but lost its significance in multivariate analysis.

Tumour response

Tumour response following SBRT is often heralded by a reduction in tumour enhancement on CT or magnetic resonance imaging (MRI) particularly in the first four months post-treatment and is usually followed by a decrease in overall tumour volume (20). Treated tumours typically show lower density compared to the adjacent liver parenchyma. In the study by Herfarth *et al.*, tumour volume of controlled tumours decreased to a median of 27% (range 0–74%) of the baseline volume. In the portal-venous phase, controlled tumours also showed a lower density than the radiation reaction [median difference against non-irradiated liver –64 HU (range, –15 to –100 HU); median difference against irradiated liver –50 HU (range, –14 to –115 HU)].

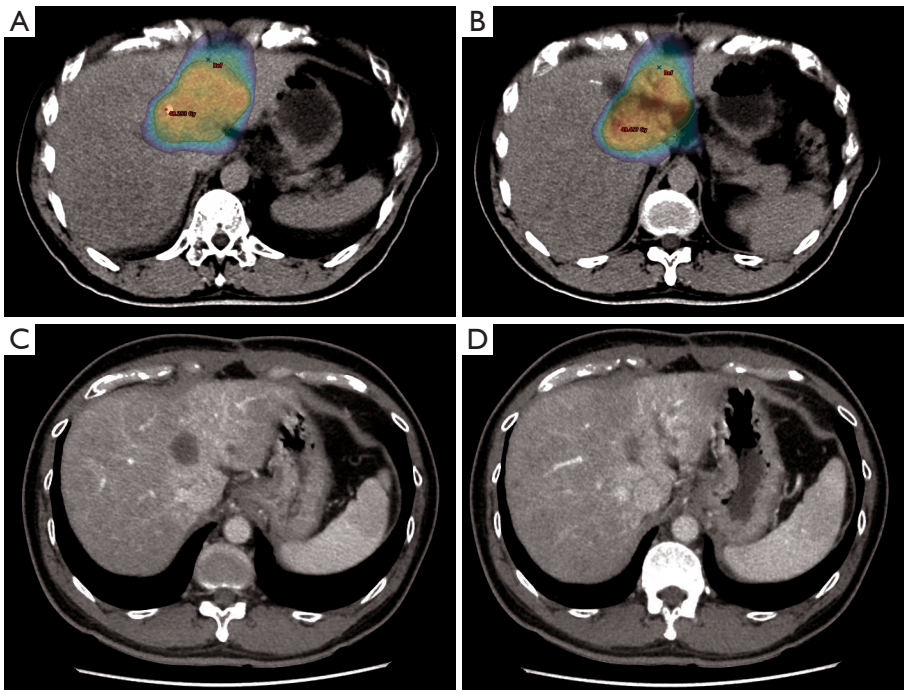

Figure 1 Radiotherapy plan showing the treated liver encompassed by 30 Gy in a patient with Child-Pugh A cirrhosis who was previously treated with TACE for a segment 4 HCC and subsequently had SBRT (40 Gy in 5 fractions) to the tumour thrombi (A,B), and CT liver in the portal-venous phase at 2 months after SBRT showing the FLR which corresponded to the area which received 30 Gy (C,D). TACE, transarterial chemoembolization; HCC, hepatocellular carcinoma; SBRT, stereotactic body radiotherapy; FLR, focal liver reaction.

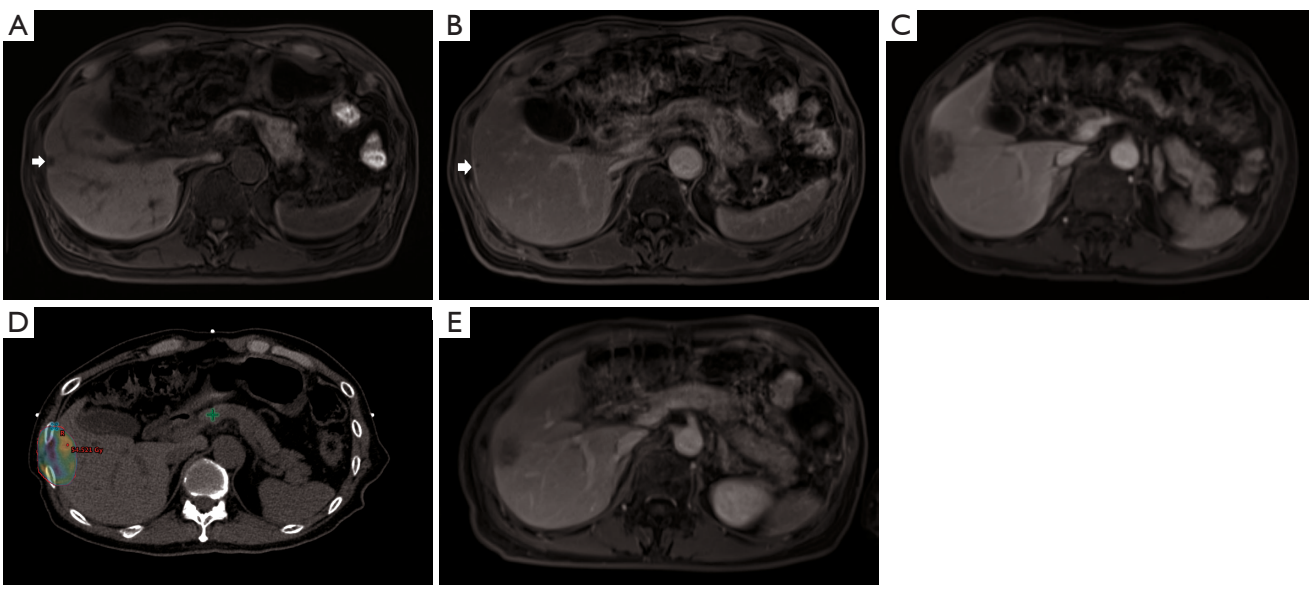

Figure 2 MRI liver with gadoxetic acid showing a segment 5 liver metastasis from nasopharyngeal cancer with focal liver reaction and no evidence of tumour recurrence. (A) Baseline pre-contrast T1-weighted MRI; (B) baseline post-contrast T1-weighted MRI showing faint peripheral enhancement after chemotherapy (white arrow); (C) post-contrast T1-weighted MRI at 5 months post-SBRT showing a hypointense and non-enhancing lesion corresponding to the (D) treated lesion covered by the 50 Gy isodose line on the planning CT; and (E) smaller hypointense and non-enhancing lesion at 12 months post-SBRT. MRI, magnetic resonance imaging; SBRT, stereotactic body radiotherapy.

Furthermore, blood vessels were not compressed or displaced by benign radiation reaction (12). The percentage of intratumoral necrosis was shown to be greater than the percentage of unidimensional size reduction in treated tumours up to 12 months post-SBRT (21). In addition, a halo of delayed enhancement can be observed in the liver parenchyma adjacent to the tumour, likely secondary to fibrosis (20). These characteristics are observed in primary liver HCC, metastases and cholangiocarcinomas treated with SBRT.

Separate imaging assessment criteria have been proposed for HCC such as the modified RECIST (mRECIST) and EASL methods which take into account tumour necrosis after local therapy (22,23). These criteria are used for both CT and MRI assessments. Both the mRECIST and EASL criteria measure the diameter of the viable arterially enhancing tumour component, rather than the whole tumour volume which includes the necrotic or non-enhancing components. The key difference between the two criteria is that the mRECIST method uses unidimensional measurement as opposed to the EASL method which uses product of bidimensional diameters. Nonetheless, the two criteria showed good concordance and has good prognostic value in HCC treated with locoregional therapy (24). The percentage of tumour necrosis has been shown to increase up to 12 months in controlled primary liver tumours treated with SBRT (21). Using these criteria, more radiological complete responders are identified compared to size-based evaluation in the portal-venous phase as per RECIST 1.1 (21). Nonetheless, RECIST 1.1 should still be considered in non-enhancing tumours or those with atypical enhancement. Another caveat is that these criteria have only been evaluated in HCC treated with non-radiotherapy modalities. Whether these are applicable to liver metastases and/or HCC treated with SBRT is still uncertain.

The development of lobulated enhancement on CT/MRI after SBRT is associated with local relapse in liver metastases (25,26). A thick (>1 mm) peripheral enhancement with at least three lobulations was found to have a sensitivity of 89%, specificity of 100%, positive predictive value of 100%, negative predictive value of 95% and accuracy of 97% in predicting local disease progression. Lobulated enhancement also preceded size-based progression in half of the cases with confirmed local progression (median delay 3.2 months). The 1-year progression-free survival (PFS) was higher in lesions without lobulated enhancement (HR 0.80; 95% CI: 0.65–0.89) compared to lesions with lobulated enhancement (HR 0.69; 95% CI: 0.54–0.80; P<0.001). This pattern of enhancement can be reliably identified between different observers with a concordance rate of 98% (26). The same group proposed a combined response criteria incorporating RECIST 1.1, necrosis and lobulated enhancement characteristics for liver metastases treated with SBRT (25). Using the combined criteria, 18% of patients were classified as complete responders as compared to 4% using the RECIST criteria. Two progressive diseases and two partial responses as determined by RECIST were classified as complete responses using the combined criteria.

Magnetic resonance imaging including diffusion-weighted (DW) imaging is increasingly used in the diagnosis and follow-up of liver tumours. DW-MRI and its quantitative parameter, the apparent diffusion coefficient (ADC) measure the rate of diffusion (Brownian motion) of water molecules within a tissue which can be restricted by cellular structures such as cell membranes, and thus could be a surrogate measurement for cellularity (27). Areas of high cellularity with resultant restricted diffusion show low ADC values compared to areas with low cellularity which gives relatively high ADC values.

In a preliminary study by Eccles *et al.*, eleven patients (4 HCCs, 5 liver metastases and 2 cholangiocarcinomas) who were treated with SBRT (28.8–54 Gy in 6 fractions) underwent DW-MRI before treatment, week 1 and week 2 of radiotherapy and at 1 month post-SBRT (28). The authors found that the mean ADC of tumours increased significantly at week 1 ($1,890\times10^{-3}$ mm/s), week 2 ($1,911\times10^{-3}$ mm/s) and 1 month ($2,011\times10^{-3}$ mm/s) compared to baseline ($1,558\times10^{-3}$ mm/s, P<0.0001). There was no significant change in the ADC values of the unirradiated liver receiving less than 8 Gy. In addition, there was no significant T2-weighted volumetric change during this interval.

In a separate study, the additional predictive value of DW-MRI in conjunction with conventional MRI using gadoxetic acid, a hepatocyte-specific contrast agent in diagnosing residual viable HCC after SBRT was evaluated (29). The mean interval between the end of treatment and follow-up MRI was 28 months (range, 2.3–57.1 months). Overall, viable tumours showed hyperintensity in T2-weighted and arterial phase images (55%), hypointensity on portal (76%), 3-minute late (66%) and hepatobiliary phase (79%) images compared to irradiated liver (*Figure 3*). In contrast, 93% of viable tumours showed hyperintensity on DW images and hypointensity on ADC maps compared to irradiated liver

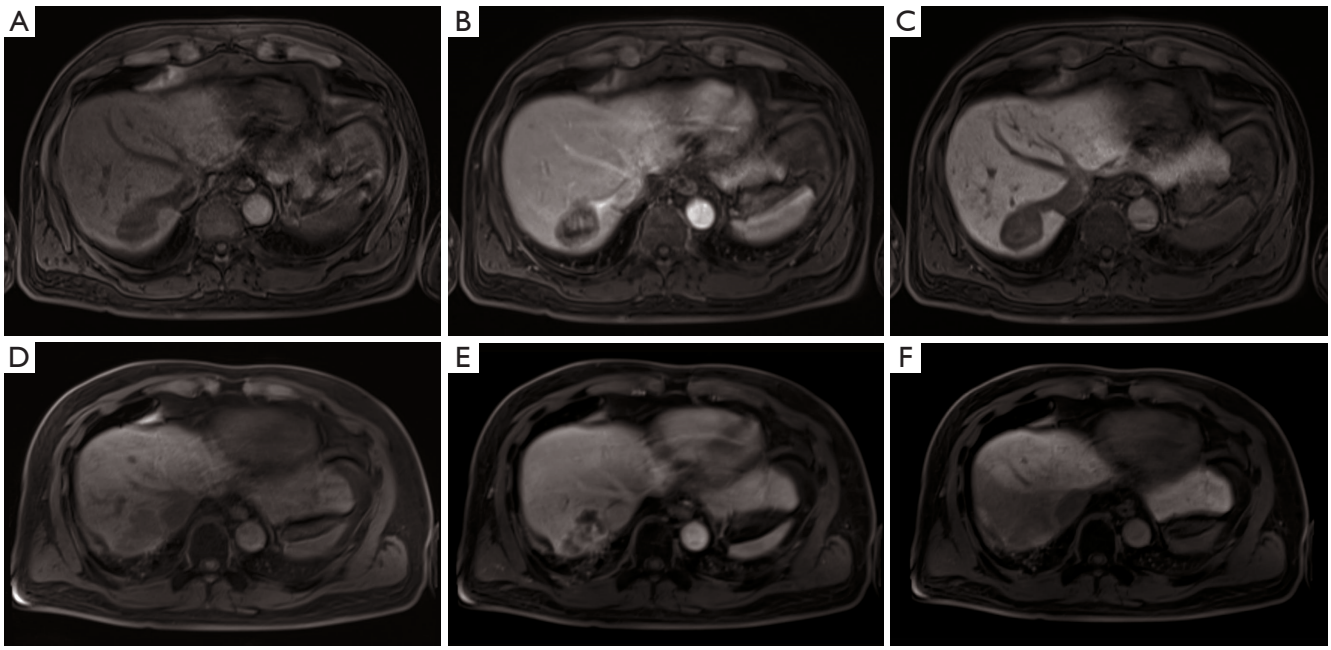

Figure 3 MRI liver with gadoxetic acid showing a recurrent segment 7 liver metastasis from colon cancer before (A-C) and 10 months after SBRT 50 Gy in 5 fractions (D-F). (A) Baseline pre-contrast T1-weighted MRI; (B) baseline post-contrast T1-weighted MRI showing tumour enhancement; (C) baseline T1-weighted hepatobiliary phase MRI showing lack of contrast uptake; (D) post-treatment pre-contrast T1-weighted MRI; (E) post-treatment post-contrast T1-weighted MRI showing peripheral and internal tumour enhancement; and (F) post-treatment T1-weighted hepatobiliary phase MRI showing lack of contrast uptake in the tumour. SBRT, stereotactic body radiotherapy; MRI, magnetic resonance imaging.

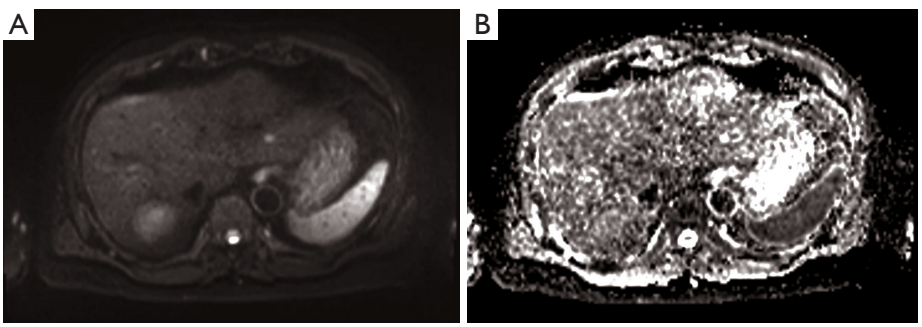

Figure 4 DW-MRI of a segment 7 colorectal liver metastasis. (A) DW image (b50) showing high signal intensity and the corresponding (B) ADC parametric map showing some intratumoral restricted diffusion. DW, diffusion-weighted; MRI, magnetic resonance imaging; ADC, apparent diffusion coefficient.

(*Figure 4*). The diagnostic performance using the area under the curve (AUC) (0.798–0.805 *vs.* 0.936–0.957) and the interobserver agreement (κ 0.450 *vs.* 0.748) were improved with the addition of DW-MRI to conventional MRI in the identification of viable tumours.

Yu *et al.* evaluated the role of DW-MRI in predicting local progression after SBRT for HCC compared to RECIST 1.1 and mRECIST in 48 patients (30). Follow-up MRI was performed between 3 to 5 months after treatment. Similar to the previous study by Park *et al.*, the authors found good interobserver agreement for region-of-interest (ROI) volumes (intraclass correlations 0.84

and 0.85) and ADC values (intraclass correlations 0.87 and 0.80) before and after radiotherapy. Both mRECIST (P<0.001) and ADC increment after SBRT (P=0.020) were significant prognostic factors for local progression-free survival (LPFS). The mRECIST criteria showed better diagnostic performance for LPFS (AUC 0.765) compared to RECIST 1.1 (AUC 0.635). However, the addition of ADC to RECIST 1.1 (AUC 0.745) had comparable diagnostic performance to mRECIST.

These results are promising but do not support the use of DW-MRI as a standard response assessment tool yet. Most of the studies included small number of patients with short follow-up, and used different acquisition parameters (e.g., b-values) and ROI definitions. In addition, tumour response was determined radiologically with limited follow-up, and without histological confirmation as it is often difficult to obtain repeat biopsy in these cases.

The use of [^{18}F]FDG PET/CT is still limited in the staging and response assessment of liver tumours, particularly HCC. Nonetheless, a few studies have evaluated the use of [^{18}F]FDG PET/CT in liver metastases treated with SBRT (11,31). The standardised uptake value (SUV) is commonly used to quantify FDG uptake within tumours. SUV_{max} is the highest value derived from a single voxel within a ROI. It was estimated that the time taken for the intratumoral SUV_{max} to decrease by 50% following liver SBRT was 2 months. The median post-treatment SUV_{max} in controlled tumour was 3.1 (range, 2.1–5.8) in one study which was reached at approximately 5 months post-SBRT. An intratumoral SUV_{max} greater than 6 after SBRT was considered as local failure if a prior post-SBRT SUV_{max} was less than 6 (11).

Conclusions

In conclusion, it is common to observe imaging changes in the adjacent irradiated normal liver after SBRT which is likely related to the underlying histopathological changes with a transient decrease in liver volume, with these changes possibly affected by the patients' underlying liver function. Intratumoral necrosis, lack of thick lobulated enhancement and subsequent tumour volume reduction are features suggestive of tumour response after SBRT. CT remains the standard method of assessing response post SBRT and we would recommend the use of multiphasic CT as the initial follow-up imaging assessment. Other imaging modalities such as DW-MRI and [^{18}F]FDG PET/CT may be useful adjunct response assessment tools demonstrating a reduction in DWI signal, an increase in ADC and a decrease in SUV if further evaluation is required. Hence, liver-specific MRI or [^{18}F]FDG PET/CT may be used if the initial CT findings are difficult to interpret (e.g., presence of fiducial markers) and/or to confirm the suspicion of tumour recurrence. We will suggest a 3-monthly imaging evaluation in the first year after SBRT followed by 6-monthly evaluation thereafter.

Acknowledgements

GJ Cook, K Owczarczyk and V Goh are supported by financial support from the Department of Health via the National Institute of Health Research Biomedical Research Centre award to Guy's and St Thomas' NHS Foundation Trust in partnership with King's College London and King's College Hospital NHS Foundation Trust; the Comprehensive Cancer Imaging Centre funded by the Cancer Research UK and Engineering and Physical Sciences Research Council in association with the Medical Research Council and Department of Health.

Footnote

Conflicts of Interest: The authors have no conflicts of interest to declare.

References

1. Lo SS, Fakiris AJ, Chang EL, et al. Stereotactic body radiation therapy: a novel treatment modality. Nat Rev Clin Oncol 2010;7:44-54.
2. Hoyer M, Roed H, Traberg Hansen A, et al. Phase II study on stereotactic body radiotherapy of colorectal metastases. Acta Oncol 2006;45:823-30.
3. Lee MT, Kim JJ, Dinniwell R, et al. Phase I study of individualized stereotactic body radiotherapy of liver metastases. J Clin Oncol 2009;27:1585-91.
4. Huertas A, Baumann AS, Saunier-Kubs F, et al. Stereotactic body radiation therapy as an ablative treatment for inoperable hepatocellular carcinoma. Radiother Oncol 2015;115:211-6.
5. Wahl DR, Stenmark MH, Tao Y, et al. Outcomes After Stereotactic Body Radiotherapy or Radiofrequency Ablation for Hepatocellular Carcinoma. J Clin Oncol 2016;34:452-9.
6. Kim MS, Kim W, Park IH, et al. Radiobiological mechanisms of stereotactic body radiation therapy

and stereotactic radiation surgery. Radiat Oncol J 2015;33:265-75.
7. Reed GB Jr, Cox AJ Jr. The human liver after radiation injury. A form of veno-occlusive disease. Am J Pathol 1966;48:597-611.
8. Fajardo LF, Colby TV. Pathogenesis of veno-occlusive liver disease after radiation. Arch Pathol Lab Med 1980;104:584-8.
9. Lawrence TS, Robertson JM, Anscher MS, et al. Hepatic toxicity resulting from cancer treatment. Int J Radiat Oncol Biol Phys 1995;31:1237-48.
10. Olsen CC, Welsh J, Kavanagh BD, et al. Microscopic and macroscopic tumor and parenchymal effects of liver stereotactic body radiotherapy. Int J Radiat Oncol Biol Phys 2009;73:1414-24.
11. Stinauer MA, Diot Q, Westerly DC, et al. Fluorodeoxyglucose positron emission tomography response and normal tissue regeneration after stereotactic body radiotherapy to liver metastases. Int J Radiat Oncol Biol Phys 2012;83:e613-8.
12. Herfarth KK, Hof H, Bahner ML, et al. Assessment of focal liver reaction by multiphasic CT after stereotactic single-dose radiotherapy of liver tumors. Int J Radiat Oncol Biol Phys 2003;57:444-51.
13. Howells CC, Stinauer MA, Diot Q, et al. Normal liver tissue density dose response in patients treated with stereotactic body radiation therapy for liver metastases. Int J Radiat Oncol Biol Phys 2012;84:e441-6.
14. Park MJ, Kim SY, Yoon SM, et al. Stereotactic body radiotherapy-induced arterial hypervascularity of non-tumorous hepatic parenchyma in patients with hepatocellular carcinoma: potential pitfalls in tumor response evaluation on multiphase computed tomography. PLoS One 2014;9:e90327.
15. Schefter TE, Kavanagh BD, Timmerman RD, et al. A phase I trial of stereotactic body radiation therapy (SBRT) for liver metastases. Int J Radiat Oncol Biol Phys 2005;62:1371-8.
16. Takeda A, Oku Y, Sanuki N, et al. Dose volume histogram analysis of focal liver reaction in follow-up multiphasic CT following stereotactic body radiotherapy for small hepatocellular carcinoma. Radiother Oncol 2012;104:374-8.
17. Yamasaki SA, Marn CS, Francis IR, et al. High-dose localized radiation therapy for treatment of hepatic malignant tumors: CT findings and their relation to radiation hepatitis. AJR Am J Roentgenol 1995;165:79-84.
18. Sanuki-Fujimoto N, Takeda A, Ohashi T, et al. CT evaluations of focal liver reactions following stereotactic body radiotherapy for small hepatocellular carcinoma with cirrhosis: relationship between imaging appearance and baseline liver function. Br J Radiol 2010;83:1063-71.
19. Kimura T, Takahashi S, Takahashi I, et al. The Time Course of Dynamic Computed Tomographic Appearance of Radiation Injury to the Cirrhotic Liver Following Stereotactic Body Radiation Therapy for Hepatocellular Carcinoma. PLoS One 2015;10:e0125231.
20. Brook OR, Thornton E, Mendiratta-Lala M, et al. CT Imaging Findings after Stereotactic Radiotherapy for Liver Tumors. Gastroenterol Res Pract 2015;2015:126245.
21. Price TR, Perkins SM, Sandrasegaran K, et al. Evaluation of response after stereotactic body radiotherapy for hepatocellular carcinoma. Cancer 2012;118:3191-8.
22. Lencioni R, Llovet JM. Modified RECIST (mRECIST) assessment for hepatocellular carcinoma. Semin Liver Dis 2010;30:52-60.
23. Bruix J, Sherman M, Llovet JM, et al. Clinical management of hepatocellular carcinoma. Conclusions of the Barcelona-2000 EASL conference. European Association for the Study of the Liver. J Hepatol 2001;35:421-30.
24. Vincenzi B, Di Maio M, Silletta M, et al. Prognostic Relevance of Objective Response According to EASL Criteria and mRECIST Criteria in Hepatocellular Carcinoma Patients Treated with Loco-Regional Therapies: A Literature-Based Meta-Analysis. PLoS One 2015;10:e0133488.
25. Jarraya H, Mirabel X, Taieb S, et al. Image-based response assessment of liver metastases following stereotactic body radiotherapy with respiratory tracking. Radiat Oncol 2013;8:24.
26. Jarraya H, Borde P, Mirabel X, et al. Lobulated enhancement evaluation in the follow-up of liver metastases treated by stereotactic body radiation therapy. Int J Radiat Oncol Biol Phys 2015;92:292-8.
27. Koh DM, Collins DJ. Diffusion-weighted MRI in the body: applications and challenges in oncology. AJR Am J Roentgenol 2007;188:1622-35.
28. Eccles CL, Haider EA, Haider MA, et al. Change in diffusion weighted MRI during liver cancer radiotherapy: preliminary observations. Acta Oncol 2009;48:1034-43.
29. Park HJ, Kim SH, Jang KM, et al. Added value of diffusion-weighted MRI for evaluating viable tumor of hepatocellular carcinomas treated with radiotherapy in patients with chronic liver disease. AJR Am J Roentgenol

2014;202:92-101.
30. Yu JI, Park HC, Lim DH, et al. The role of diffusion-weighted magnetic resonance imaging in the treatment response evaluation of hepatocellular carcinoma patients treated with radiation therapy. Int J Radiat Oncol Biol Phys 2014;89:814-21.
31. Solanki AA, Weichselbaum RR, Appelbaum D, et al. The utility of FDG-PET for assessing outcomes in oligometastatic cancer patients treated with stereotactic body radiotherapy: a cohort study. Radiat Oncol 2012;7:216.

Cite this article as: Yip C, Cook GJ, Owczarczyk K, Goh V. Challenges in imaging assessment following liver stereotactic body radiotherapy: pitfalls to avoid in clinical practice. Chin Clin Oncol 2017;6(Suppl 2):S11. doi: 10.21037/cco.2017.06.06

